Nanotubes-Assembled Pine-Needles-Like CuS as Effective Energy Booster for Sodium-Ion Storage

Dongxu Yu[a†], Malin Li[a,b†], Tong Yu[c†], Chunzhong Wang[a], Yi Zeng[d,*], Xiaodong Hu[e], Gang Chen[a], Guochun Yang[c,*], and Fei Du[a,*]

[a]Key Laboratory of Physics and Technology for Advanced Batteries (Ministry of Education), College of Physics, Jilin University, Changchun, 130012, People's Republic of China

[b]State Key Laboratory of Inorganic Synthesis and Preparative Chemistry, College of Chemistry, Jilin University, Changchun, 130012, People's Republic of China

[c]Center for Advanced Optoelectronic Functional Materials Research and Key Laboratory for UV Light-Emitting Materials and Technology of Ministry of Education and Department of Chemistry, Northeast Normal University, Changchun 130024, China

[d]College of Materials Science and Engineering, Jilin University, Changchun, 130012, People's Republic of China

[e]Department of Materials Engineering, The University of British Columbia, Vancouver, Canada

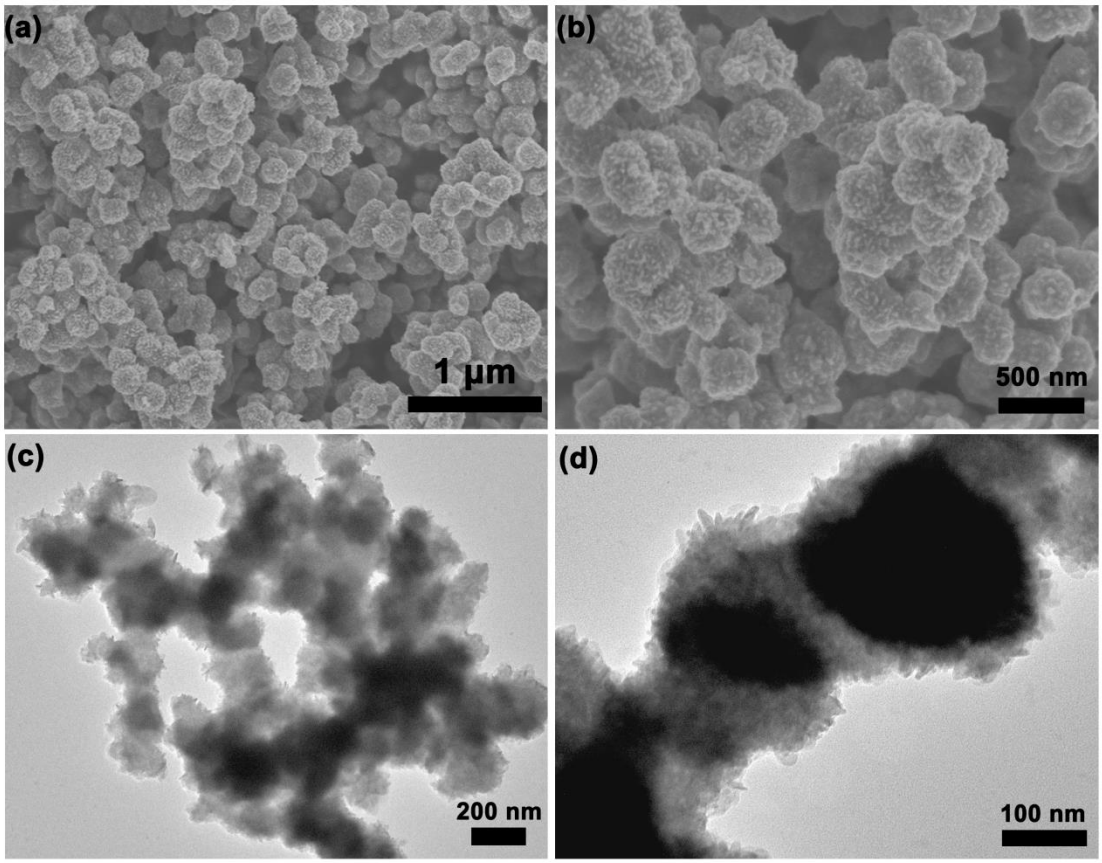

Fig. S1. FESEM images (a, b) and TEM images (c, d) of I-CuS.

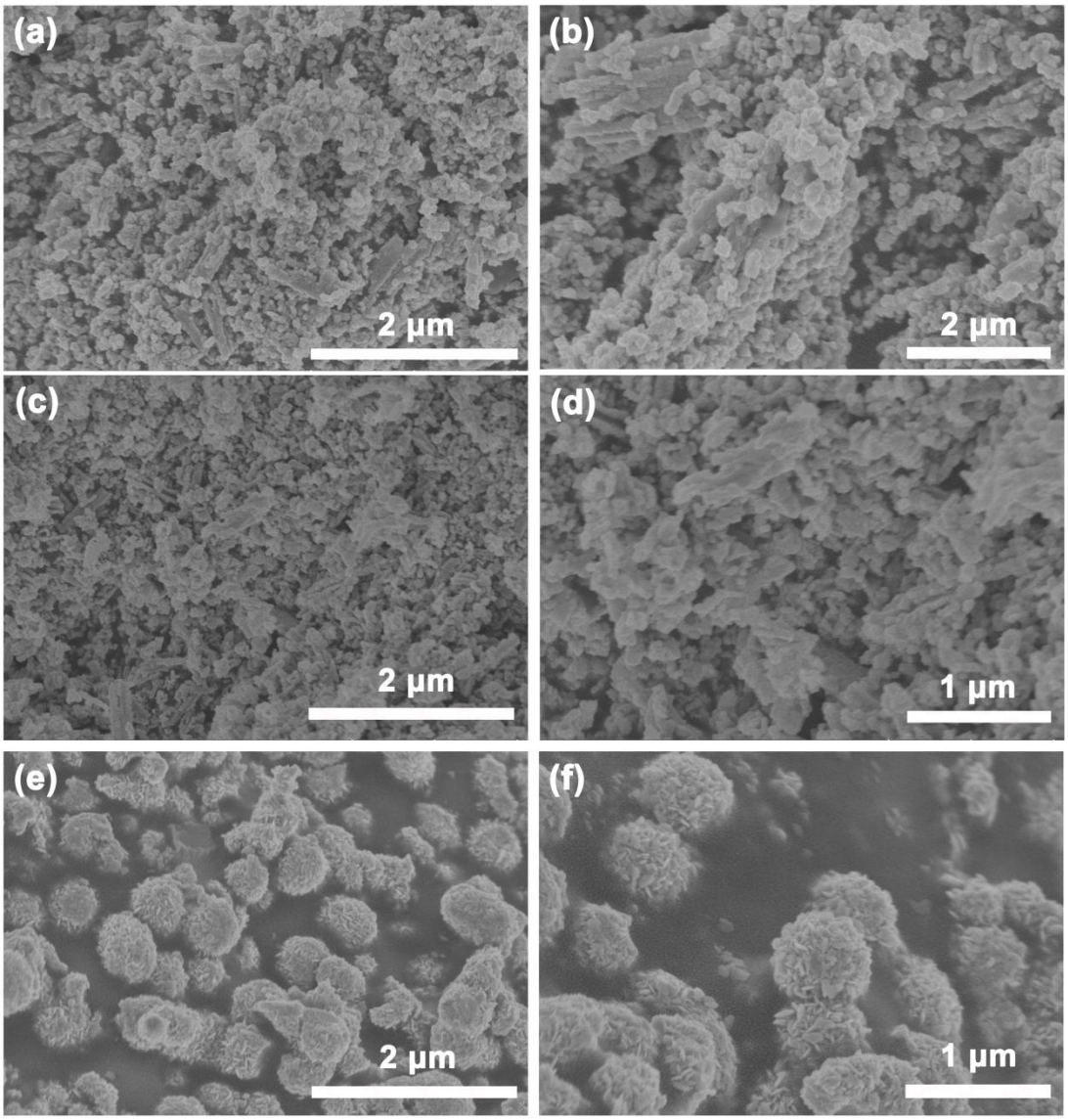

Fig. S2. FESEM images of the samples synthesized with different solvent. (a, b) mixture of 20 mL EG and 20 mL H_2O. (c, d) mixture of 10 mL EG and 30 mL H_2O. (e, f) 40 mL H_2O.

By further decreasing the content of EG, the viscosity and the chelation of the solvent are also decreased, causing fast nucleation and aggregation growth of the CuS nanocrystal. Thus, there is no sufficient time for the nanocrystal to find the low-energy configuration interface and form perfectly oriented aggregations (as shown in **Fig. S2a-d**). When perform the preparation with pure H_2O as the mono-solvent, the morphology of the product resemble that using EG as the solvent. Apparently, the content and the ratio of the solvent is an essential part for the fabrication of various morphologies.

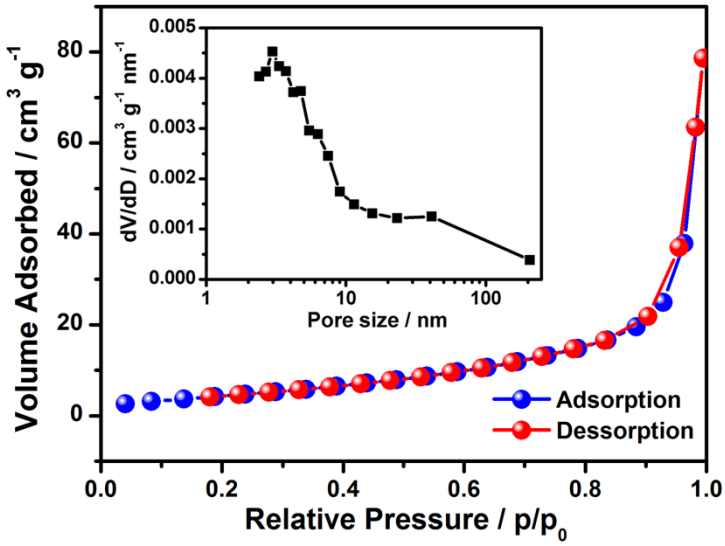

Fig. S3. N_2 adsorption-desorption isotherm and pore-size distribution (inset) of PNL-CuS.

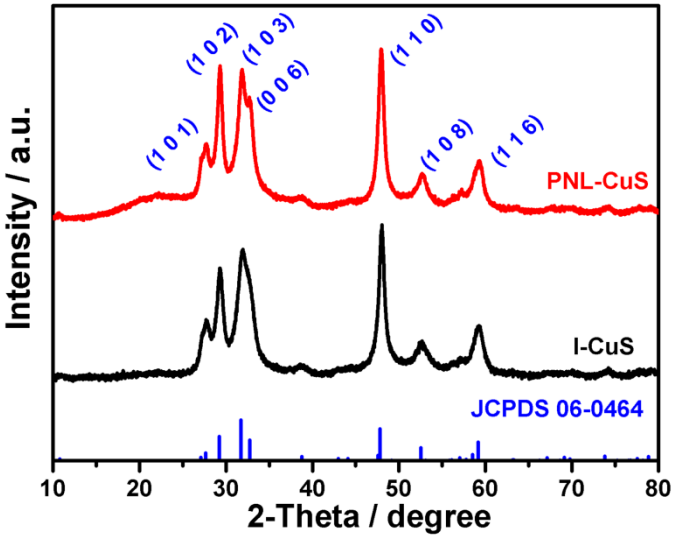

Fig. S4. XRD patterns of I-CuS and PNL-CuS.

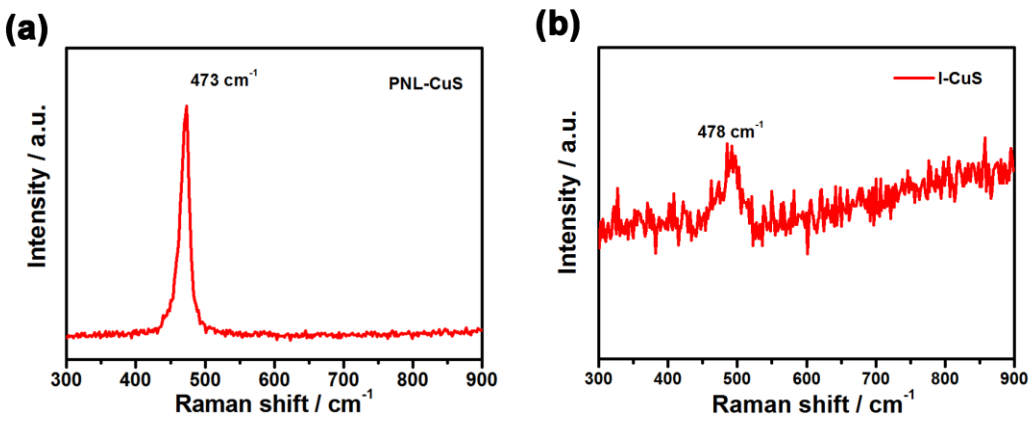

Fig. S5. Raman spectrum of the as-prepared PNL-CuS and I-CuS

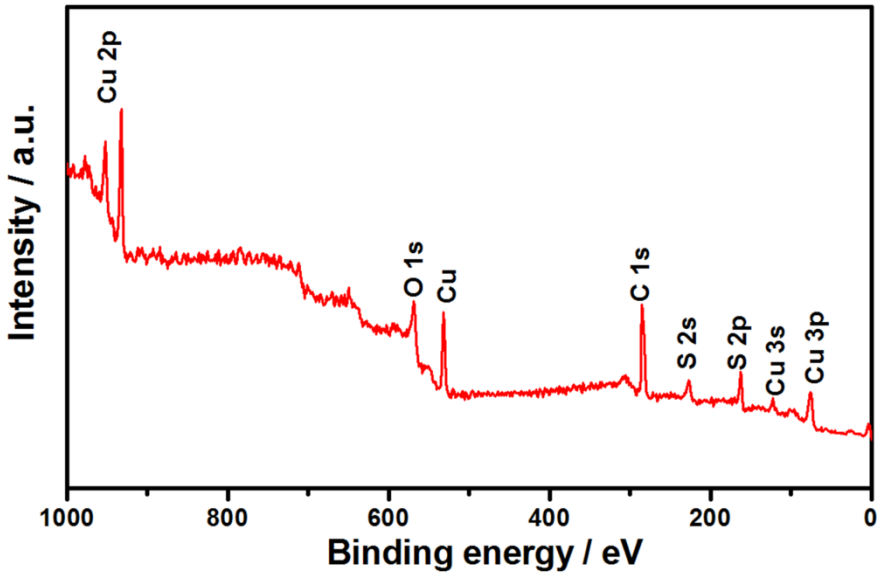

Fig. S6. XPS survey spectrum of PNL-CuS.

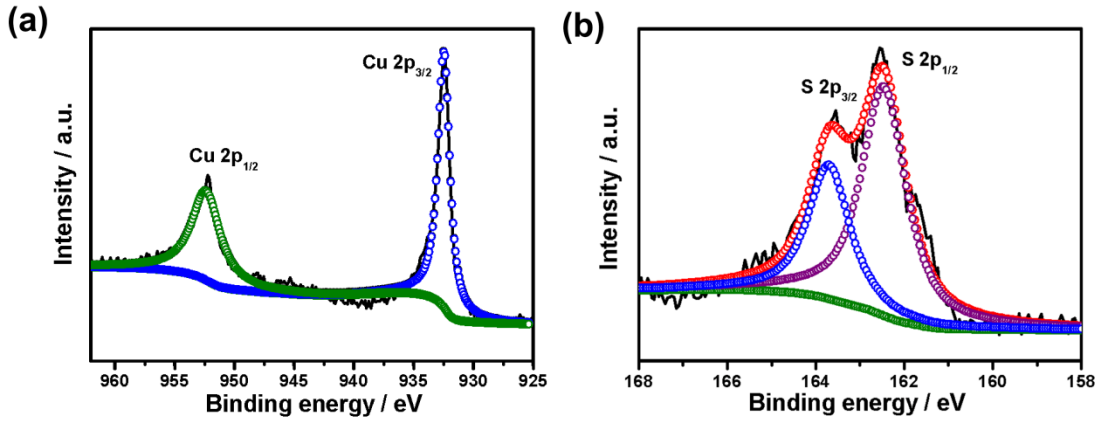

Fig. S7. High-resolution XPS spectra of (a) Cu 2p and (b) S 2p of PNL-CuS.

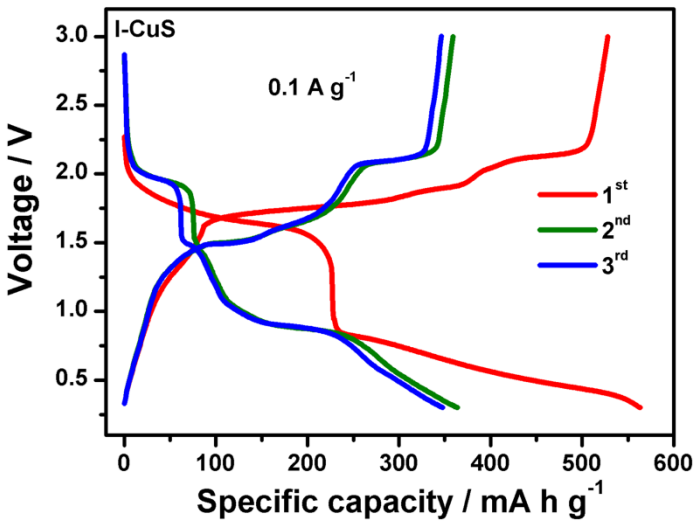

Fig. S8. Galvanostatic discharge-charge curves of I-CuS at 0.1 A g^{-1}.

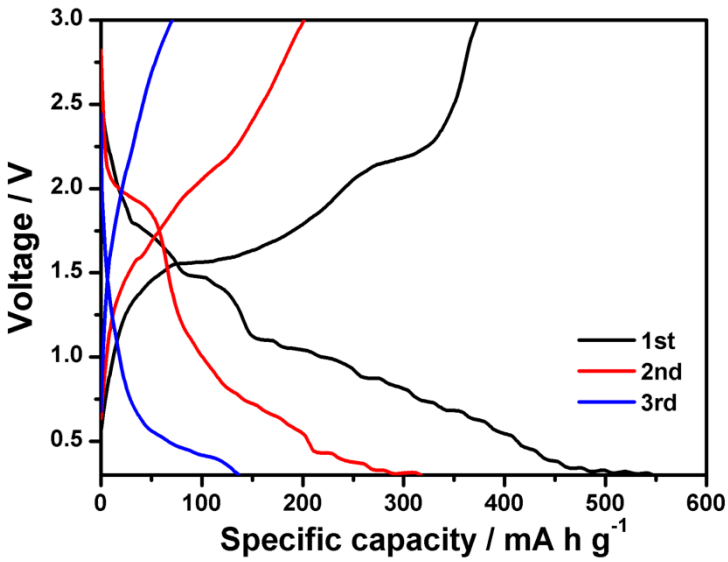

Fig. S9. Galvanostatic discharge-charge curves of PNL-CuS by using ester-based electrolyte (1M $NaClO_4$ in PC:EC=1:1vol.%) in the voltage range of 0.3-3.0 V.

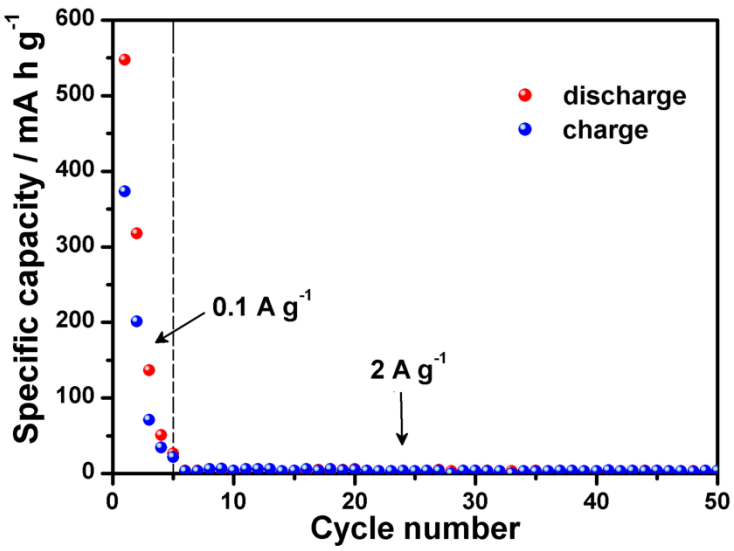

Fig. S10. Cycling performance of PNL-CuS between 0.3 and 3.0 V by using ester-based electrolyte at 2 A g^{-1} with activation at 0.1 A g^{-1} for first 5 cycles.

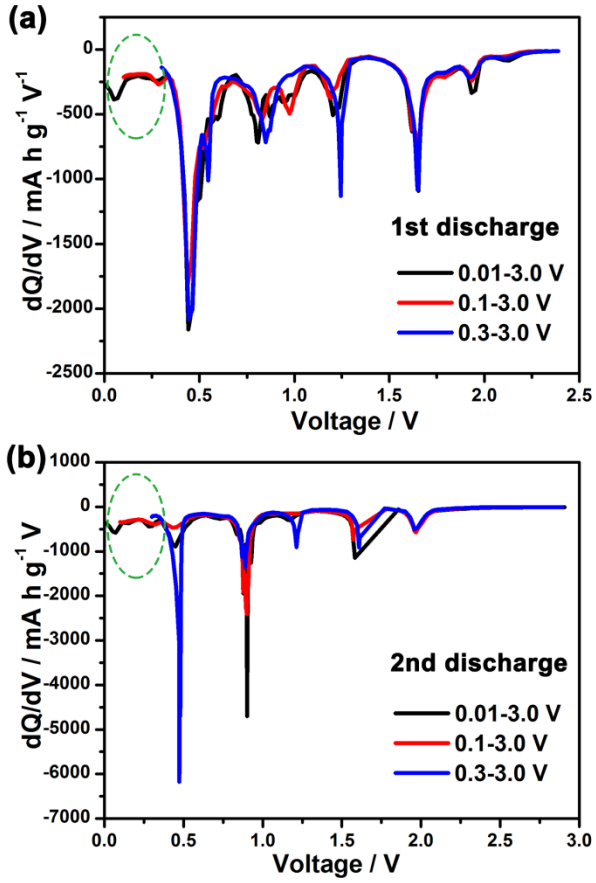

Fig. S11. dQ/dV profiles of PNL-CuS in various voltage ranges for **(a)** the 1st and **(b)** the 2nd discharging processes by using ether-based electrolyte**.**

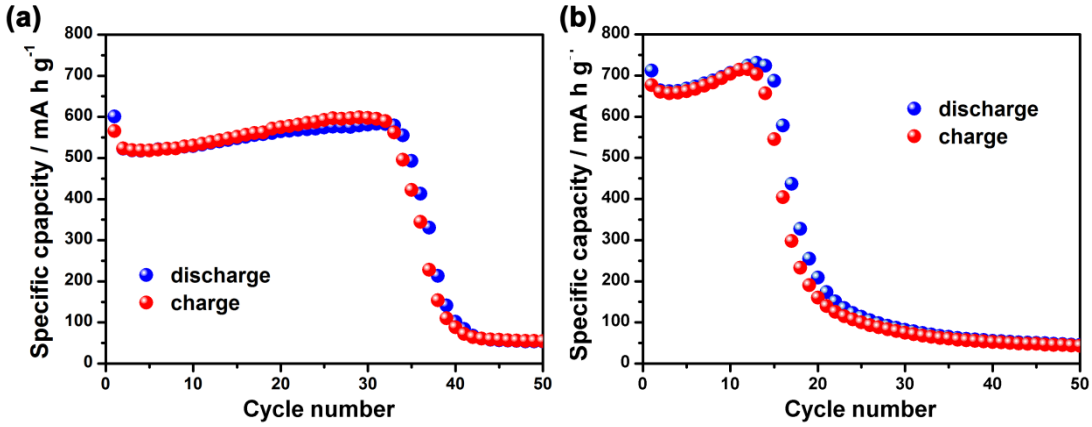

Fig. S12. Cycling performance of PNL-CuS in the voltage range of **(a)** 0.1-3.0 V, and **(b)** 0.01-3.0 V by using ether-based electrolyte.

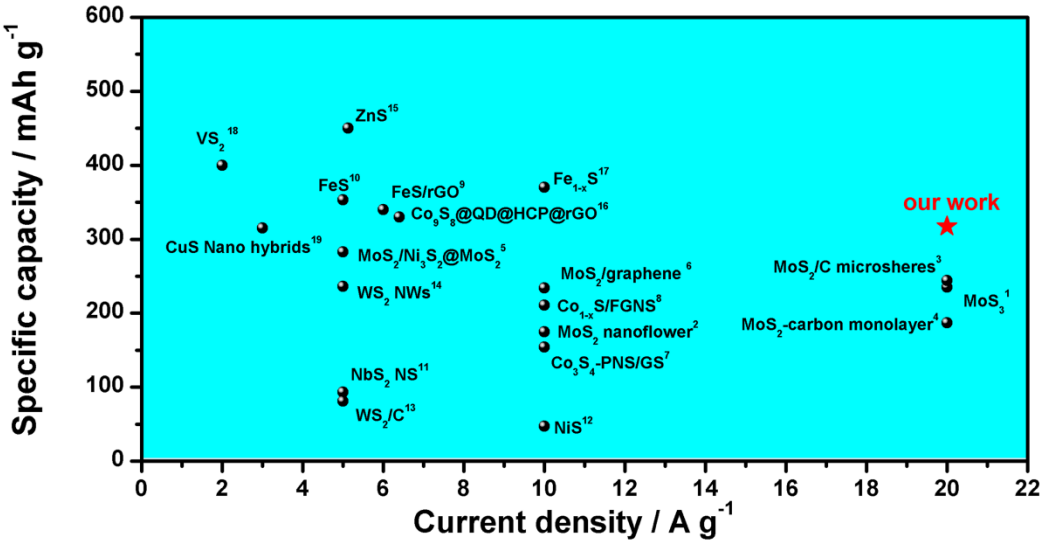

Fig. S13. Rate capabilities of PNL-CuS compared with other published metal sulfides as anode of sodium-ion batteries.

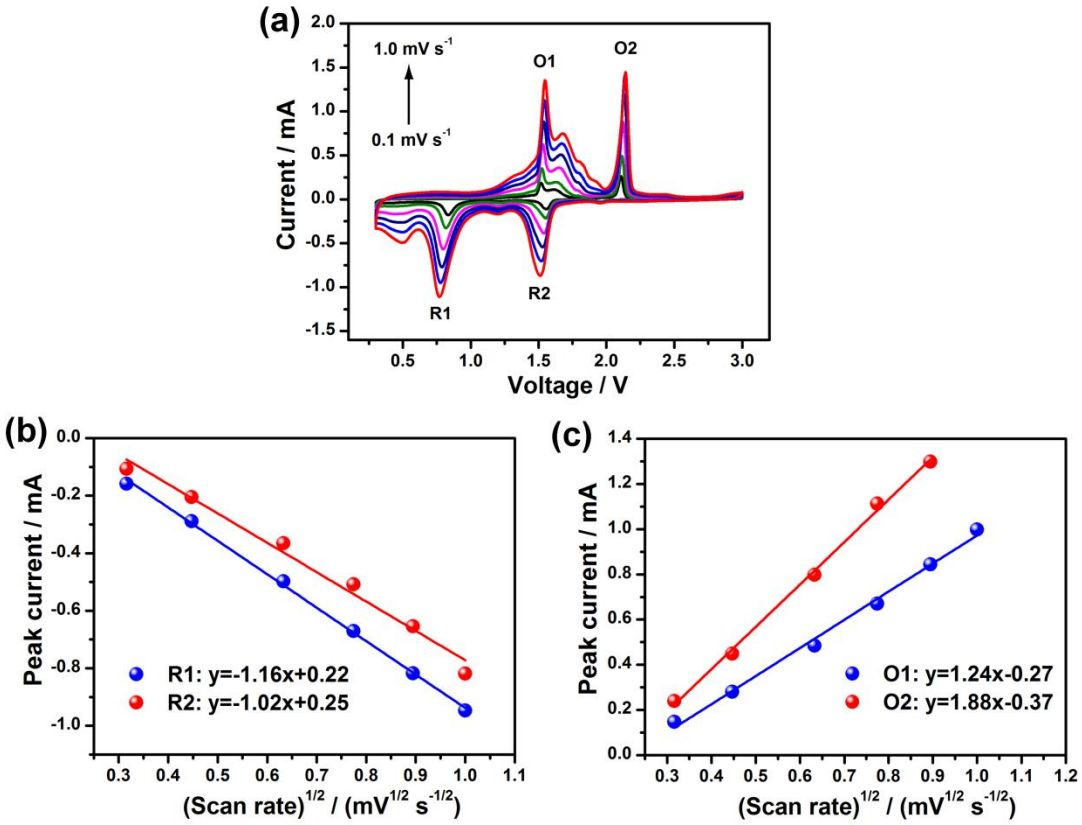

Fig. S14. (a) CV curves of I-CuS at various scan rates. **(b, c)** Linear relationship between peak currents (I_p) and the square root of the scan rate ($v^{1/2}$) with the corresponding linear fits.

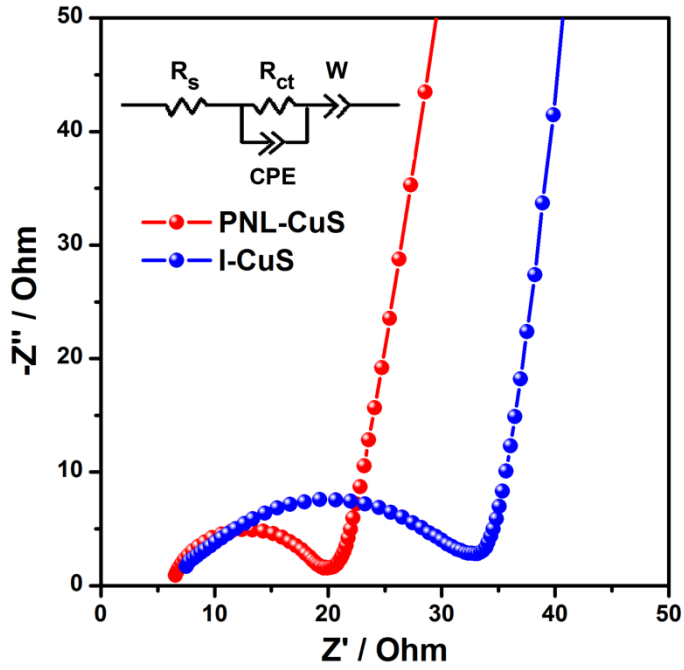

Fig. S15. Nyquist plots of PNL-CuS and I-CuS after the initial charge process. The inset displays the equivalent circuit for fitting, where R_s presents the internal resistance, R_{ct} presents the charge-transfer resistance, and W presents the Warburg impedance.

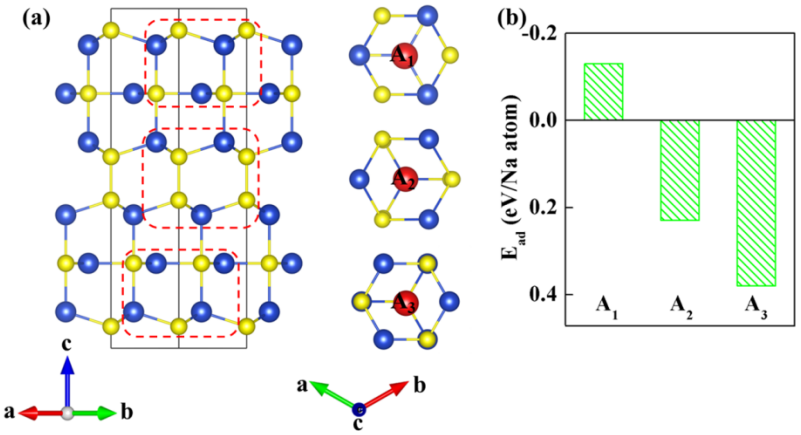

Fig. S16. (a) Based on the structural character of bulk CuS, there are three possible adsorption sites. A_1 is in the center of Cu_4S_6-dodecagon, A_2 sits in the middle of Cu_4S_6-dodecagon with S-S bond, A_3 is in the center of Cu_6S_4-dodecagon. (b) The calculated adsorption energy of the three different inequivalent adsorption sites. Here, the site with negative adsorption energy prefers to the adsorption of the Na ions. Thus, A_1 is stable adsorption site for Na ion and can occur spontaneous.

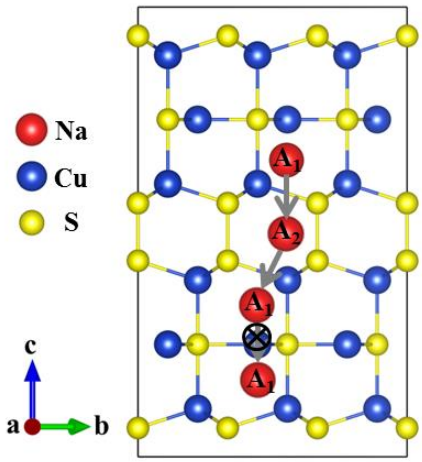

Fig. S17. Path II of Na ions diffusion in CuS.

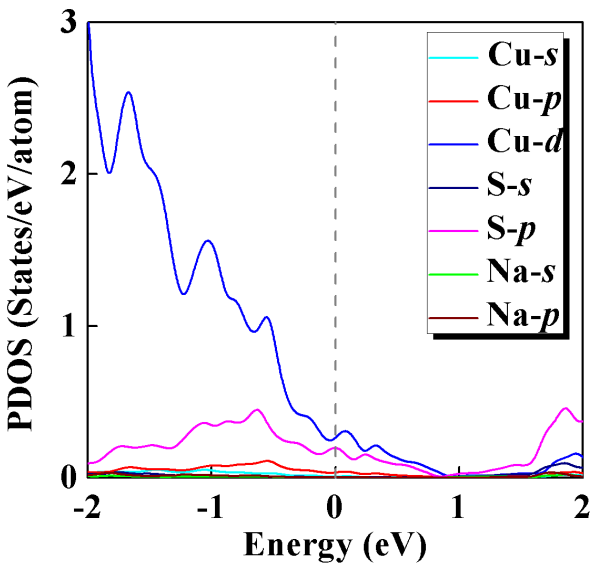

Fig. S18. Calculated partial density of states of one Na ion adsorbed in A_1 site of CuS.

Table S1. Na^+ diffusion coefficient of PNL-CuS and I-CuS calculated from O1, O2, R1, and R2.

Sample	R1 (cm^2 s^{-1})	R2 (cm^2 s^{-1})	O1 (cm^2 s^{-1})	O2 (cm^2 s^{-1})
PNL-CuS	5.41×10^{-11}	4.56×10^{-10}	1.68×10^{-11}	5.61×10^{-10}
I-CuS	3.93×10^{-11}	4.39×10^{-10}	1.65×10^{-11}	4.89×10^{-10}

Table S2. Fitted impedance parameters of PNL-CuS and I-CuS after the initial charge process.

Sample	R_s (Ω)	R_{ct} (Ω)
PNL-CuS	6.15	12.6
I-CuS	6.34	26.1

Reference:

[1] H. Ye, L. Wang, S. Deng, X. Zeng, K. Nie, P. N. Duchesne, B. Wang, S. Liu, J. Zhou, F. Zhao, N. Han, P. Zhang, J. Zhong, X. Sun, Y. Li , Y. Li, J. Liu, *Adv. Energy Mater.* 2017, **7**, 1601602.

[2] Z. Hu, L. Wang, K. Zhang, J. Wang, F. Cheng, Z. Tao, J. Chen, *Angew. Chem. Int. Ed*. 2014, **126**, 13008-13012.

[3] Y. Lu, Q. Zhao, N. Zhang, K. Lei, F. Li, J. Chen, *Adv. Funct. Mater.* 2016, **26**, 911-918.

[4] Z-T. Shi, W. Kang, J. Xu, Y.-W. Sun, M. Jiang, T.-W. Ng, H.-T. Xue, D.Y.W. Yu, W. Zhang, C.-S. Lee, *Nano Energy* 2016, **22**, 27-37.

[5] J. Wang, J. Liu, H. Yang, D. Chao, J. Yan, S. V. Savilov, J. Lin, Z.X. Shen, *Nano Energy* 2016, **20**, 1-10.

[6] S.H. Choi, Y.N. Ko, J.-K. Lee, Y.C. Kang, *Adv. Funct. Mater.* 2015, **25**, 1780-1788.

[7] Y. Du, X. Zhu, X. Zhou, L. Hu, Z. Dai, J. Bao, *J. Mater. Chem. A.* 2015, **3**, 6787-6791.

[8] T. Chen, Y. Ma, Q. Guo, M. Yang, H. Xia, *J. Mater. Chem. A.* 2017, **5**, 3179-3185.

[9] S.Y. Lee, Y.C. Kang, *Chem. Eur. J.* 2016, **22**, 2769-2774.

[10] J.S. Jung, J.-S. Park, Y.C. Kang, *Nano Res.* 2017, **10**, 897-907.

[11] X. Ou, X. Xiong, F. Zheng, C. Yang, Z. Lin, R. Hu, C. Jin, C. Yu, M. Liu, *J. Power Sour.* 2016, **325**, 410-416.

[12] Y. Wang, D. Kong, W. Shi, B. Liu, G. J. Sim, Q. Ge, H. Y. Yang, *Adv. Energy Mater*. 2016, **6**, 161057.

[13] C. Zhu, P. Kopold, W. Li, P. A. Aken, J. Maier. Y. Yu, *J. Mater. Chem. A.* 2015, **3**, 20487-20493.

[14] Y. Liu, N. Zhang, H. Kang, M. Shang, L. Jiao, J. Chen, *Chem. Eur. J.* 2015, **21**, 11878-11884.

[15] D. Su, K. Kretschmer, G. Wang, *Adv. Energy Mater.* 2016, **6**, 1501785.

[16] Z. Chen, R. Wu, M. Liu, H. Wang, H. Xu, Y. Guo, Y. Song, F. Fang, X. Yu, D.

Sun, *Adv. Funct. Mater.* 2017, **27**, 1702046.

[17] L. Li, S. Peng, N. Buncher, H.-Y. Chen, N. Shen, A. Nagasubramanian, E. Eldho, S. Hartung, S. Ramakrishna, M. Srinivasan, *Nano Energy,* 2017, **37**, 81-89.

[18] J. Zhou, L. Wang, M. Yang, J. Wu, F. Chen, W. Huang, N. Han, H. Ye, F. Zhao, Y. Li, Y. Li, *Adv. Mater.* 2017, 1702061.

[19] N. R. Kim, J. Choi, H. J. Yoon, M. E. Lee, S. U. Son, H.-J. Jin, Y. S. Yun, *Acs Sustain Chem. Eng.* 2017, **5**, 9802-9808.